Fast timing on XEUS

L. Strüder[a], D. Barret[b], C. Fiorini[c], E. Kendziorra[d], P. Lechner[e]

[a] Max-Planck-Institut für extraterrestrische Physik, Giessenbachstr., D-85741 Garching, Germany
[b] Centre d'Etude Spatiale des Rayonnements, Av. du Colonel Roche 9, F-31028 Toulouse, France
[c] Politecnico di Milano, Piazza Leonardo da Vinci 32, I-20133 Milano, Italy
[d] Eberhard-Karls-Universität, Wilhelmstr. 7, D-72074 Tübingen, Germany
[e] PNSensor GmbH, Römerstr. 28, D-80803 München, Germany

ABSTRACT

Fast X-ray timing observations are a method to probe strong gravity fields around compact massive objects. The European X-ray Evolving Universe Spectroscopy (XEUS) mission with its large collecting area telescope will be able to deliver the required extremely good photon statistics for these studies. The fast timing detector in the focal plane must be able to operate at up to 10^7 incoming photons from the brightest X-ray objects in the sky with an energy resolution of 200 eV FWHM at 5.9 keV at a dead time not exceeding 1 % and a time resolution of 10 µsec. Silicon Drift Detectors (SDDs) with their extremely small value of the readout capacitance have proved that they can handle high count rates with simultaneous good energy resolution. For the XEUS fast timing detector it is proposed to operate a multi-channel SDD at an out of focus position to distribute the flux of photons over a number of detector cells.

1. SCIENTIFIC BACKGROUND

The X-rays generated in the inner accretion flows around black holes and neutron stars carry information about regions of the strongly curved space-time in the vicinity of these objects. This is a regime in which there are important predictions of general relativity still to be tested. High resolution X-ray spectroscopy and fast timing studies can both be used to diagnose the orbital motion of the accreting matter in the immediate vicinity of the collapsed star, where the effects of strong gravity become important.

With the discovery of millisecond aperiodic X-ray time variability (or so-called quasi-periodic oscillations) from accreting black holes and neutron stars, and brightness burst oscillations in neutron stars, the Rossi X-ray Timing Explorer (RXTE) has clearly demonstrated that fast X-ray timing has the potential to measure accurately the motion of matter in strong gravity fields and to constrain masses and radii of neutron stars, and hence the equation of state of dense matter [1].

The X-ray Evolving Universe Spectroscopy mission (XEUS) is designed to perform imaging and spectroscopic observations of the furthest X-ray sources to trace the origin and evolution of hot matter back to the early ages of the universe [2]. To achieve this goal, XEUS requires a huge collecting area. The same requirement applies to fast X-ray timing studies, for which extremely good photon statistics is needed. In view of its mirror aperture, XEUS will provide an improvement of more than one order of magnitude in sensitivity for timing studies over RXTE. XEUS will enable for the first time the testing of predictions of general relativity in strong gravity fields, such as frame dragging effects and fully relativistic periastron precession. In addition, XEUS will allow to study the waveform of coherent brightness X-ray burst oscillations in detail. The waveform is directly affected by gravitational light deflection and relativistic Doppler shifts, and yields direct constraints on the mass and radius of the neutron star, and hence the equation of state of its high density core. The properties of the neutron star cores have been the subject of considerable speculation, and remain a major issue in modern physics. Similarly, the modeling of the waveform of the high frequency quasi-periodic oscillations, which will for the first time be observed on their coherence time scales, can place important constraints on the mass and spin of the black hole.

A fast timing capability on XEUS would also extend its field of applications, by allowing the study of the X-ray variability of a wide class of objects, such as low-mass X-ray binaries in external galaxies, accreting and isolated pulsars, accreting white dwarfs, and X-ray transients, especially the so-called micro-quasars. Accretion and jet formation are crucial in understanding aspects of astrophysics from normal stars to super-massive black holes. The fast timing

capability can be combined with good energy resolution and broad band coverage allowing time resolved spectroscopic observations. For instance, the space-time geometry close to black holes could be probed using variability in the Fe-K_α line.

2. DETECTOR REQUIREMENTS

The detector requirements are derived from the ability of the fast timing capability to observe the brightest X-ray sources in the sky, mostly X-ray binaries, either transient or persistent. Simulations using the specified values of the effective area of the XEUS mirror [3] show that the Crab would produce about 250 kilo-counts per sec (kcps) and about 800 kcps in XEUS phase A and B, i.e. with an effective mirror area of 6 m² and 30 m² at 1 keV, respectively. Sco X-1, bright transients and X-ray bursts can be ten times brighter. This leads to a requirement to be able to handle up to 3 mega-counts per sec (Mcps) in phase A and 10 Mcps in phase B. In addition, the arrival time of each photon should be recorded with a timing resolution of about 10 µsec, and the dead time should not exceed 1%. The energy resolution of the detector should be around 200 eV FWHM at 5.9 keV, i.e. a factor of 10 improvement over current instrumentation for timing studies. Finally, the detector energy range should cover the high-energy response of the mirrors, as timing signals tend to become stronger at higher energies.

3. THE SILICON DRIFT DETECTOR

3.1 Device principle

The Silicon Drift Detector (SDD) is derived from the principle of sideward depletion [4]. The idea is that a large area semiconductor wafer, e.g. of high-resistivity n-type silicon, is covered by large area p^+ junctions on both surfaces. In reverse bias of the p^+ junctions with respect to a small sized n^+ ohmic contact depletion layers expand from the p^+ layers into the n-type bulk with the square root of the applied voltage. Both depletion zones propagate until, at a given voltage, they touch each other and the entire device is depleted at a voltage four times lower than that needed to deplete a conventional p^+nn^+ diode of the same thickness. In that condition the electron potential energy in a cross section perpendicular to the surface of the device has a parabolic shape with a minimum in the center plane.
In an SDD an electric field with a strong component parallel to the wafer surface is superposed to the sideward depletion structure. The direction of the field is such that electrons released within the depleted volume by thermal generation or by the absorption of ionizing radiation are forced to drift to the small-sized n^+ bulk contact, which acts as charge collecting anode. The SDD principle combines a large depleted volume for the absorption of ionizing radiation with a small value of the anode capacitance, the precondition for collection and readout of the signal electrons with minimum serial noise contribution.
In the original SDD design the electric field is achieved by segmentation of the p^+ regions on both surfaces to patterns of parallel strips [4]. To optimize the SDD concept for X-ray spectroscopy the strip system on both surfaces is replaced by a large area p^+ junction on the side opposite to the n^+ anode [5]. This non-structured p^+ junction is used as a homogeneous,

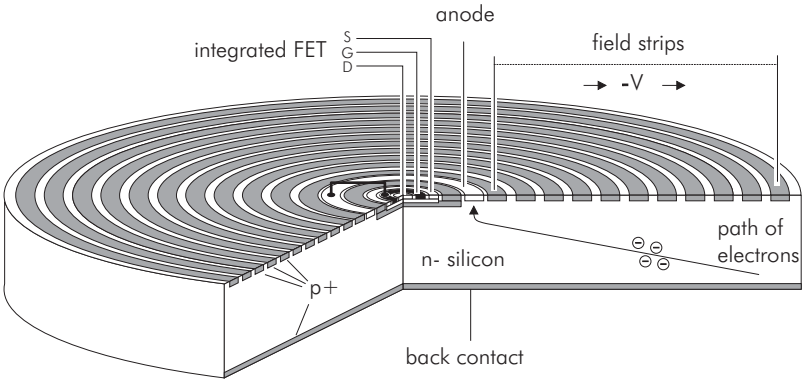

Figure 1

Circular SDD with uniform radiation entrance window. The entire thickness of the device is sensitive to radiation. The first FET of the amplifying electronics is integrated in the center of the ring-shaped anode.

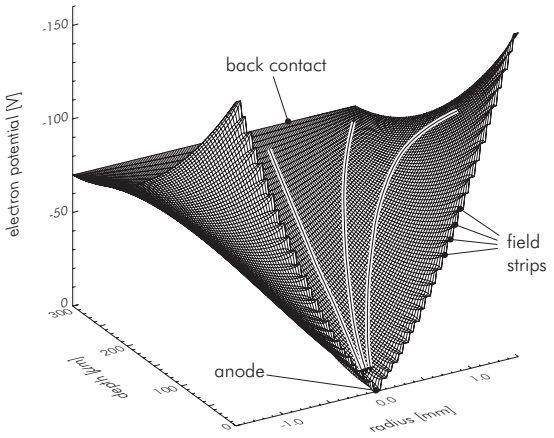

Figure 2

Calculated distribution of the potential energy in an SDD. The simulation applies to the cross section of a detector as shown in fig. 1. The arrow lines indicate the signal electrons' drift directions.

thin radiation entrance window. In addition backside illumination has a self-shielding effect: the radiation sensitive components, e.g. the readout structure, are placed on the non-irradiated surface and can only be hit by hard X-rays (> 10 keV), whose intensity is reduced by the absorption of the silicon bulk. A further improvement is the design of circular, concentric drift electrodes driving signal electrons to the small sized n^+ anode in the center of the device. The potential values of the drift rings are defined by an integrated voltage divider, i.e. only the inmost and the outmost rings must be biased externally [6].

With the SDD topology and the collecting anode's small physical size the detector contribution to the total readout capacitance is already minimized. An additional reduction is achieved by the integration of the first transistor of the amplifying electronics on the detector chip [7]. The integrated transistor is a single-sided n-JFET [8, 9, 10] designed to operate on a fully depleted n-type bulk. It is placed in the center of the ring shaped collecting anode (fig. 1). The anode is connected to the floating FET gate by a narrow metal strip, so that the change of the anode voltage caused by signal electrons can be easily measured as a modulation of the transistor current. The on-chip FET has an internal, self-adapting discharging mechanism [11], so that there is no need for an externally clocked reset pulse, and the whole system is working with dc-voltages only. The integration of the first FET not only minimizes the overall capacitance recommending the SDD for high-resolution, high-rate spectroscopy, but also makes it insensitive to a great extent against electronic pickup and microphony, i.e. noise induced by mechanical vibration.

Figure 1 shows the topology of an SDD with cylindrical geometry, uniform entrance window, and integrated FET. Figure 2 shows the corresponding calculated potential energy distribution.

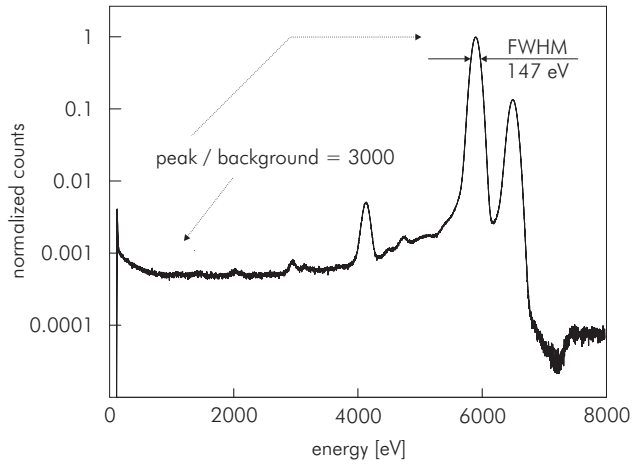

Figure 3

Spectrum of a radioactive ^{55}Fe source obtained with a 10 mm² SDD at -10 °C. The energy resolution in terms of FWHM at the Mn-K_α line is 147 eV, the peak/background ratio is 3000.

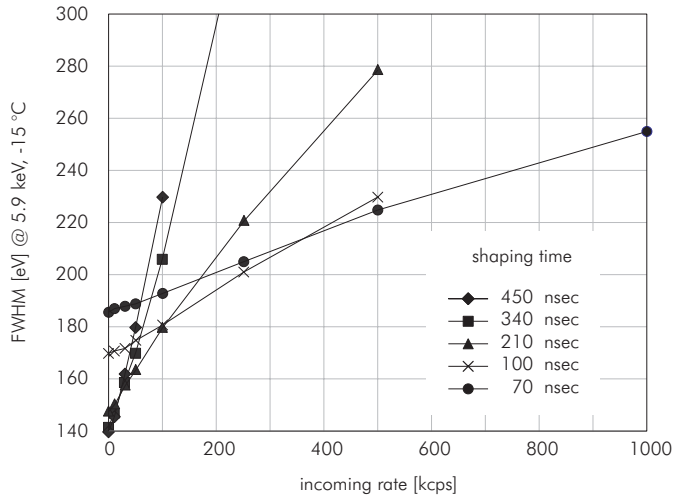

Figure 4

Measured count rate dependent energy resolution of an SDD with analog pulse processing system at a temperature of -15 °C. With the shortest shaping time of 70 nsec the system is still able to operate at 10^6 incoming photons per sec with a throughput of $4 \cdot 10^5$ processed counts per sec.

3.2 SDD performance

SDDs of the type shown in fig. 1 have been fabricated and qualified at the semiconductor laboratory of the Max-Planck-Institutes for physics and for extraterrestrial physics in Munich/Germany in large quantities in different shapes and sizes. Due to the advanced process technology used in the SDD fabrication the leakage current level is so low, typically 100 pA/cm^2 at full depletion of the 300 µm thick wafer, that the devices can be operated at room temperature or with moderate cooling by a single-stage thermoelectric cooler. The numbers quoted in the following reflect the typical performance of an SDD with a sensitive area of 10 mm^2 operated at a temperature of -10 °C (14 °F).
The *energy resolution* in terms of full-width-at half-maximum (FWHM) at the Mn-K_α line (5.9 keV) is 147 eV (fig. 3). Because of the small value of the total output capacitance of about 200 fF the SDD is operated at pulse shaping time constants of the order of 100 nsec (fig. 4), whereas conventional systems with comparable spectroscopic quality require longer shaping times by about a factor of 100. This means that the SDD can be used at extremely high count rates far beyond the ability of other systems. Figure 4 demonstrates the *count rate capability* obtained by an analog pulse processing system with variable shaping time constant [12]. With a shaping time of 70 nsec the energy resolution is still

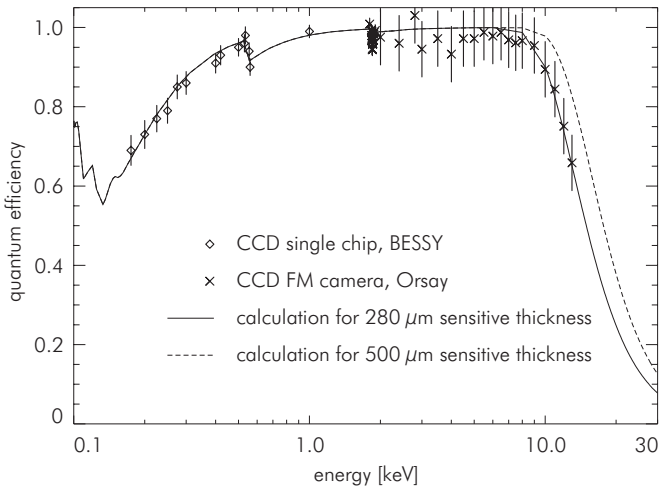

Figure 5

Measured (discrete points) and calculated (solid line) quantum efficiency of pn-CCDs [15]. Because of identical technology and material the curves are also valid for SDDs. The dashed line at the high energy end indicates the improvement of quantum efficiency due the increase of the sensitive thickness from 280 µm to 500 µm.

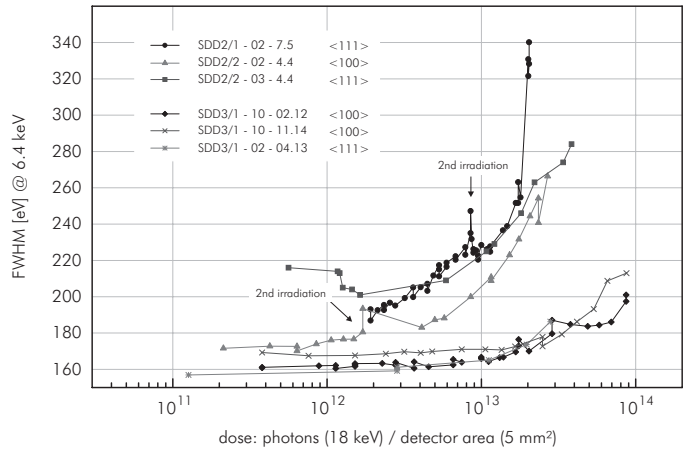

Figure 6

SDD energy resolution in terms of FWHM at 6.4 keV as function of the number of absorbed 18 keV photons for two device generations. The actual SDDs (SDD3 generation, lower 3 curves) show no radiation damage effect up to 10^{13} absorbed photons.

better than 260 eV (FWHM at 5.9 keV) at 10^6 incoming photons per sec and a throughput of $4 \cdot 10^5$ processed counts per sec. For high energy resolution at lower count rates longer shaping time constants up to 450 nsec are selected.
The radiation entrance window has been optimized for the detection of soft X-rays [13, 14]. The *quantum efficiency* is above 90% in the energy range from 300 eV up to 10 keV. On the low energy end the quantum efficiency is a function of the entrance window technology. On the high energy end it is given by the absorption properties of the fully depleted 300 µm thick silicon bulk. The comparison of measured and calculated values of the quantum efficiency (fig. 5) has actually obtained with fully depleted pn-CCDs for the XMM-Newton satellite [15], but it can be taken for SDDs as well, because it uses the same entrance window technology. The quantum efficiency at high energy will increase for the next generations of SDDs as they will be processed on 500 µm thick substrate material (fig. 5). The quality of the entrance window is also reflected in the low energy background of SDD spectra (fig. 3). The peak/background ratio defined as amplitude ratio of the Mn-K_α line relative to the average background at 1 keV is 3000.
Observing bright sources the fast timing detector on XEUS will be exposed to high radiation doses. The limitation in the maximum acceptable dose arises from high energy photons that enter through the backside window, pass the depleted bulk without interaction, and are absorbed in the oxide covering parts of the opposite surface. The generation of oxide charges and interface states will cause an increased surface generation rate of leakage current and may damage radiation sensitive components, e.g. the readout structure or the integrated voltage divider. To prove their *radiation hardness* SDDs have been irradiated with a high flux of Mo-K_α photons (17.5 keV). Photons of this energy have a maximum probability of transmission through the 300 µm thick silicon bulk and absorption in the oxide layer on the opposite surface. Figure 6 demonstrates the improvement of radiation tolerance by design and technology optimization from a previous generation of SDDs to the actual one. Irradiated devices of the actual production reveal no change in energy resolution up to 10^{13} absorbed photons [16]. Only at higher doses an increase of interface-generated leakage current is observed, a total failure of the device did not occur. That means that the SDD can be operated under worst case conditions for 3 continuous years at a constant rate of 10^5 incoming photons per sec without any radiation damage effect. The growth of the silicon bulk thickness from 300 µm to 500 µm for the next SDD generations will result in a further increase of the self-shielding effect and improved radiation hardness.

4. THE XEUS FAST TIMING DETECTOR

Although it is the fastest known X-ray spectroscopy detector, a single SDD as introduced in the previous sections cannot meet the extreme system requirements of the XEUS fast timing detector. To handle a photon rate of 1 Mcps one must therefore distribute the focal beam over ten or more detectors. The easiest solution is a monolithic array of SDDs on a single wafer. Such multi-channel SDDs already exist [17]. They consist of a continuous, gapless arrangement of a number of SDDs with individual readout, but with common voltage supply, entrance window, and guard ring structure. Multi-channel SDDs are used e.g. in fast photon counting applications at synchrotron light facilities like EXAFS [18]and X-ray holography [19], and for the optical light readout of scintillator crystals in medical imaging [20].

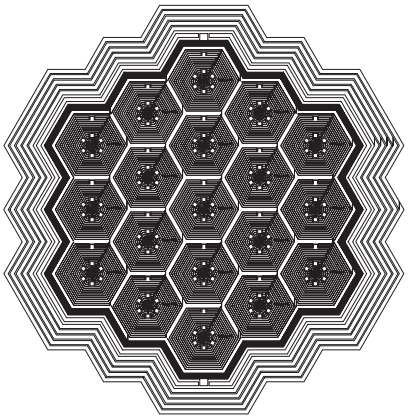

Figure 7

Multi-channel SDD with 19 hexagonal cells. The cell size is 5 mm². The cells have an individual readout, they share common a voltage supply, backside radiation entrance window, and guard ring system.

Figure 7 shows an example of a 19-cell SDD array with a cell size of 5 mm² and a total area of almost 1 cm². The single ^{55}Fe spectra of fig. 8 obtained with the 19-cell SDD at 0 °C with a pulse shaping time of 1 µsec demonstrate the almost ideal homogeneity of the device [20]. Only one cell (SDD # 8) has a reduced performance, which was presumably caused by mechanical damage during the mounting procedure. The sum spectrum with 165 eV FWHM at 5.9 keV was accomplished after a gain correction of the individual channels.

To spread the total photon flux over the SDD array the detector must be placed and operated out of focus. The necessary out of focus distance for a 1 cm² SDD array is in the order of 15 cm at a focal length of 50 m and an outer mirror diameter of about 4 m in XEUS phase A. For XEUS phase B with a mirror diameter of 10 m it reduces to 5 cm. This could be done by a fixed position above or below the other focal plane instruments in the detector spacecraft. A second option is to change the distance between the detector and the mirror spacecrafts.

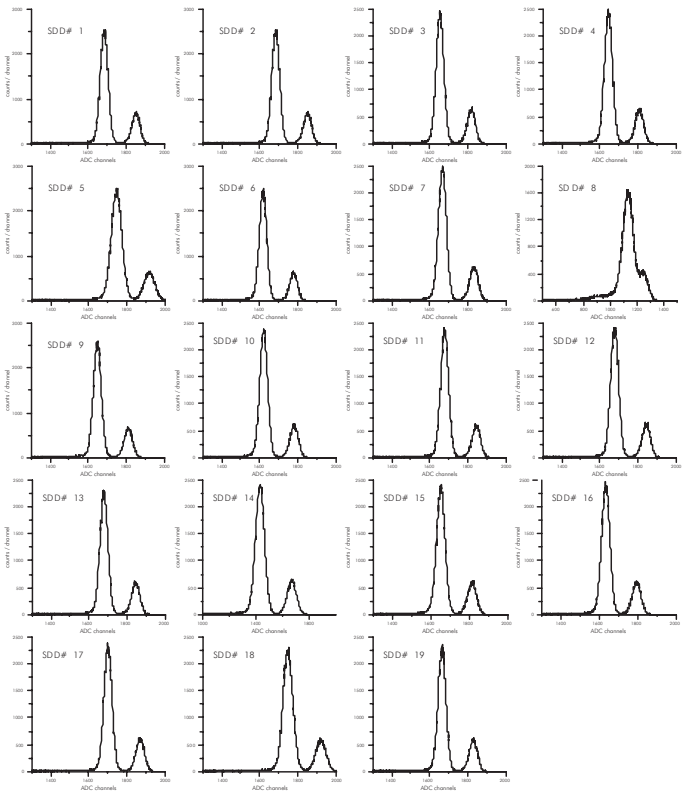

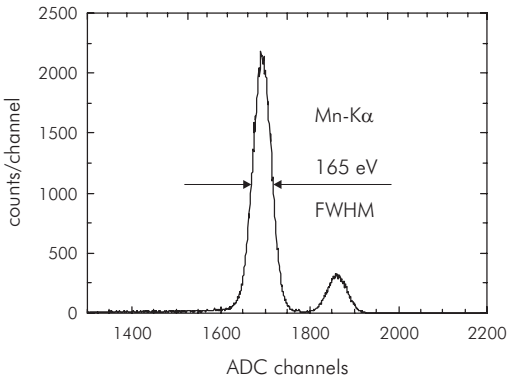

Figure 8

Spectra of a ^{55}Fe source obtained with a 19-cell SDD shown in fig. 7 at 0 °C with a filter time constant of 1 µsec [20]. The individual cells show an almost ideally homogeneous response. Only one cell (SDD # 8) has a reduced performance presumably caused by mechanical damage during mounting. The sum spectrum with 165 eV FWHM at 5.9 keV has been obtained after gain correction of the single channels.

REFERENCES

1. H.V. Bradt, R.E. Rothschild, J. H. Swank, "X-ray timing explorer mission", *Astronomy and Astrophysics Supplement Series 97(1)*, p. 355, 1993
2. The XEUS Astrophysics Working Group, "X-ray Evolving Universe Spectroscopy - The XEUS Science Case", *ESA SP-1238*, 2000
3. The XEUS Telescope Working Group, "X-ray Evolving Universe Spectroscopy - The XEUS Telescope", *ESA SP-1253*, 2001
4. E. Gatti, P. Rehak, "Semiconductor drift chamber - an application of a novel charge transport scheme", *Nucl. Instr. and Meth. A 225*, p. 608, 1984
5. J. Kemmer, G. Lutz, E. Belau, U. Prechtel, W. Welser, "Low capacity drift diode", *Nucl. Instr. and Meth. A 253*, p. 378, 1987
6. P. Lechner, L. Andricek, N. Findeis, D. Hauff, P. Holl, J. Kemmer, P. Klein, G. Lutz, N. Meidinger, E. Pinotti, R. Richter, L. Strüder, C. von Zanthier, "New DEPMOS applications", *Nucl. Instr. & Meth. A 326*, p. 284, 1993
7. P. Lechner, S. Eckbauer, R. Hartmann, S. Krisch, D. Hauff, R. Richter, H. Soltau, L. Strüder, C. Fiorini, E. Gatti, A. Longoni, M. Sampietro, "Silicon drift detectors for high resolution room temperature X-ray spectroscopy", *Nucl. Instr. and Meth. A 377*, p. 346, 1996
8. V. Radeka, P. Rehak, S. Rescia, E. Gatti, A. Longoni, P. Holl, L. Strüder, J. Kemmer, "JFET for Completely Depleted High Resistivity Silicon", *Jour. de Physique 49 (9)*, p. 363, 1988
9. V. Radeka, P. Rehak, S. Rescia, E. Gatti, A. Longoni, P. Holl, L. Strüder, J. Kemmer, "Implanted Silicon JFET on Completely Depleted High Resistivity Devices", *IEEE El. Dev. Lett. 10 (2)*, p. 91, 1989
10. E. Pinotti, H. Bräuninger, N. Findeis, H. Gorke, D. Hauff, P. Holl, J. Kemmer, P. Lechner, G. Lutz, W. Kink, N. Meidinger, G. Metzner, P. Predehl, C. Reppin, L. Strüder, J. Trümper, C. v. Zanthier, E. Kendziorra, R. Staubert, V. Radeka, P. Rehak, G. Bertuccio, E. Gatti, A. Longoni, A. Pullia, M. Sampietro, "The pn-CCD On-Chip Electronics", *Nucl. Instr. and Meth. A 326*, p. 85, 1993
11. C. Fiorini, P. Lechner, "Continuous charge restoration in semiconductor detectors by means of gate-to-drain current of the integrated front-end JFET", *IEEE Trans. Nucl. Sci. Vol. 46(3)*, p. 761, 1999
12. RÖNTEC GmbH, Berlin, Germany, *X-flash product information*, 1997
13. R. Hartmann, D. Hauff, P. Lechner, R. Richter, L. Strüder, J. Kemmer, S. Krisch, F. Scholze, G. Ulm, "Low energy response of silicon pn-junction detector", *Nucl. Instr. & Meth. A 377*, p. 191, 1996
14. R. Hartmann, L. Strüder, J. Kemmer, P. Lechner, O. Fries, E. Lorenz, R. Mirzoyan, "Ultrathin entrance windows for silicon drift detectors", *Nucl. Instr. and Meth. A 387*, p. 250, 1997
15. H. Soltau, J. Kemmer, N. Meidinger, D. Stötter, L. Strüder, J. Trümper, C. v. Zanthier, H. Bräuniger, U. Briel, D. Carathanassis, K. Dennerl, S. Engelhard, F. Haberl, R. Hartmann, G. Hartner, D. Hauff, H. Hippmann, P. Holl, E. Kendziorra, N. Krause, P. Lechner, E. Pfeffermann, M. Popp, C. Reppin, H. Seitz, P. Solc, T. Stadlbauer, U. Weber, U. Weichert, " Fabrication, test and performance of very large X-ray CCDs designed for astrophysical applications ", *Nucl. Instr. and Meth. A 439*, p. 547, 2000
16. P. Lechner, A. Pahlke, H. Soltau, accepted for publication in *X-ray Spectrometry*, 2003
17. P. Lechner, W. Buttler, C. Fiorini, R. Hartmann, J. Kemmer, N. Krause, P. Leutenegger, A. Longoni, H. Soltau, D. Stötter, R. Stötter, L. Strüder, U. Weber, "Multichannel silicon drift detectors for X-ray spectroscopy", *Proc. SPIE Vol. 4012*, p. 592, 2000
18. Ch. Gauthier, J. Goulon, E. Moguiline, A. Rogalev, P. Lechner, L. Strüder, C. Fiorini, A. Longoni, M. Sampietro, A. Walenta, H. Besch, H. Schenk, R. Pfitzner, U. Tafelmeier, K. Misiakos, S. Kavadias, D. Loukas, "A high resolution, 6-channels, silicon drift detector array with integrated JFETs designed for XAFs: first X-ray fluorescence excitation spectra recorded at the ESRF", *Nucl. Instr. and Meth. A 382*, p. 524, 1996
19. B. Adams, T. Hiort, E. Kossel, G. Materlik, Y. Nishino, D.V. Novikov, "X-ray fluorescence holography in theory and experiment", *phys. stat. sol. (b) 215*, p. 757 , 1999
20. C. Fiorini, A. Longoni , L. Boschini , F. Perotti , C. Labanti , E. Rossi , P. Lechner , L. Strüder, "Position and Energy Resolution of a new Gamma-ray Detector based on a Single CsI(Tl) Scintillator Coupled to a Silicon Drift Detector Array", *IEEE-NS 46(4)*, p. 858, 1999